Scenario development of ITER ELMy H-mode hydrogen plasma

E. Tholerus[1], L. Garzotti[1], Y. Baranov[1], G. Corrigan[1], F. Eriksson[1], D. Farina[2], L. Figini[2], D.M. Harting[3], F. Koechl[1], A. Loarte[4], E. Militello Asp[1], H. Nordman[5], V. Parail[1], S.D. Pinches[4], A.R. Polevoi[4], R. Sartori[6], P. Strand[5]

[1] *CCFE, Culham Science Centre, Abingdon, Oxon, OX14 3DB, UK*

[2] *Istituto per la Scienza e Tecnologia dei Plasmi, CNR, Milan, Italy*

[3] *Institut für Energie- und Klimaforschung IEK-4, FZJ, TEC, 52425 Jülich, Germany*

[4] *ITER Org., Route de Vinon-sur-Verdon, CS 90 046, 13067 St. Paul Lez Durance, France*

[5] *Association EURATOM-VR, Chalmers University of Technology, Göteborg, Sweden*

[6] *Fusion For Energy Joint Undertaking, Josep Pla 2, 08019, Barcelona, Spain*

Introduction

Following the ITER first plasma, ITER will undergo operation preparing for the main deuterium and deuterium–tritium campaigns [1]. During this preparatory phase, referred to as Pre-Fusion Power Operation (PFPO), stable H-mode operation will be demonstrated, and several systems, including auxiliary heating & current drive, various diagnostics, ELM mitigation, and divertor heat flux control, will be commissioned. Hydrogen and helium will be the main plasma species to ensure non-active operation.

For commissioning of the ELM mitigation systems, stable operation in type I ELMy H-mode is required. One of the scenarios suggested for this purpose is the hydrogen plasma half-field half-current baseline (7.5MA/2.65T). Auxiliary heating and current drive is done by a combination of ECRH and NBI, since there exists no efficient ICRH heating scheme for this particular scenario [2]. This results in a maximum auxiliary heating power of 53 MW (20 MW ECRH and 33 MW NBI). This paper presents integrated core, edge and SOL/divertor modelling using JINTRAC [3], developed by EUROfusion, investigating whether 53 MW of auxiliary power is sufficient for stable ELMy H-mode operation or if additional heating is required. Different techniques for lowering the L–H power threshold are also considered in the modelling.

Modelling assumptions

The assumed L–H power threshold scaling law is based on Martin08 [4], with a correction $P_{\mathrm{L-H}} = P_{\mathrm{L-H,Martin08}} \times (2/A_{\mathrm{eff}})$ for hydrogenic plasmas [5]. This scaling law is expected to deviate towards larger $P_{\mathrm{L-H}}$ when $\langle n_{\mathrm{e}} \rangle \lesssim n_{\mathrm{e,min}} \approx 0.4 n_{\mathrm{GW}} \approx 2.5 \times 10^{19}\ \mathrm{m}^{-3}$ [6]. JET experiments have shown that both $P_{\mathrm{L-H}}$ and $n_{\mathrm{e,min}}$ are sensitive to the detailed strike-point configuration [7], which is non-trivial to translate to ITER scenarios due to differences in divertor geometry. The assumed $P_{\mathrm{L-H}}$ and $n_{\mathrm{e,min}}$ is a compromise between several aspects of their respective observed

dependencies in past experiments, details of which is beyond the scope of this paper.

Two different ECRH power schemes are considered. The first scheme is 20 MW using the present design of the ITER ECRH systems. In the second scheme, 10 MW of ECRH power is added, based on an upgrade of the ITER heating systems that is being assessed [1]. JET experiments [8] have suggested that a minority of helium can reduce $P_{\mathrm{L-H}}$ of hydrogen plasmas. Therefore, we will also consider the cases with and without added helium, assuming a 15 % reduction of $P_{\mathrm{L-H}}$ when $\langle n_{\mathrm{He}} \rangle \approx 0.1 \langle n_{\mathrm{e}} \rangle$. Another option for reducing the L–H power threshold is to operate at densities close to $n_{\mathrm{e,min}} \approx 0.4 n_{\mathrm{GW}}$, as $P_{\mathrm{L-H}} \sim \langle n_{\mathrm{e}} \rangle^{0.717}$ [4]. It should be noted that recent JET experiments have shown that $n_{\mathrm{e,min}}$ for helium plasmas can range between $0.4 n_{\mathrm{GW}}$ and $0.7 n_{\mathrm{GW}}$ depending on the strike-point configuration [9]. This observation could potentially invalidate results presented here, which assumes a reduction of $P_{\mathrm{L-H}}$ by a helium minority at $\langle n_{\mathrm{e}} \rangle$ close to $0.4 n_{\mathrm{GW}} \approx 2.5 \times 10^{19}\ \mathrm{m}^{-3}$ (case C, as presented below).

In order to avoid unacceptable levels of NBI shine-through power in lower density regimes that can reduce the life expectancy of the NBI shield blocks, a neon minority can be introduced to increase the beam stopping [10]. In these simulations, neon gas rates are adapted to reach stabilised total shine-though power below about 1.8 MW while avoiding full divertor detachment.

ECRH/ECCD is modelled using GRAY [11]. The equatorial EC launchers operate in O-mode, which gives less parasitic absorption and more efficient ECCD than X-mode operation during H-mode confinement. NBI heating and current drive is modelled with PENCIL [12], operating at full power (16.5 MW on each of the two negative ion source injectors), injecting hydrogen at ∼870 keV. For impurity physics, SANCO [13] is used, and core heat and particle transport is handled by JETTO [14] and EDWM [15]. JETTO includes a continuous ELM model, which has been used with the assumption $\alpha_{\mathrm{crit}} = 1.8$ for type I ELMs, based on edge ideal MHD calculations of similar scenarios [16]. Plasma–wall/divertor interaction and scrape-off layer/private region transport and atomic physics is modelled with EDGE2D-EIRENE [17].

Results

The simulation results are presented in Fig. 1. Cases are labelled A – D according to the figure legends. The cases start with full ECRH power, adding 33 MW of NBI power at $t = 0$. In cases A & B, the NBI power was instantaneously activated at full power, whereas cases C & D do a gradual ramp-up of the NBI power over 400 ms for smoother L–H transition. All cases except case A were able to reach a stable type I ELMy H-mode, as seen in Fig. 1.a. Case D operates at a 35 – 55 % higher density than the other cases, which were kept close to the lower limit of the $P_{\mathrm{L-H}}$ high density branch (see Fig. 1.b). This was done to demonstrate the wide operational space of this particular case, which benefits both from 10 MW of additional ECRH

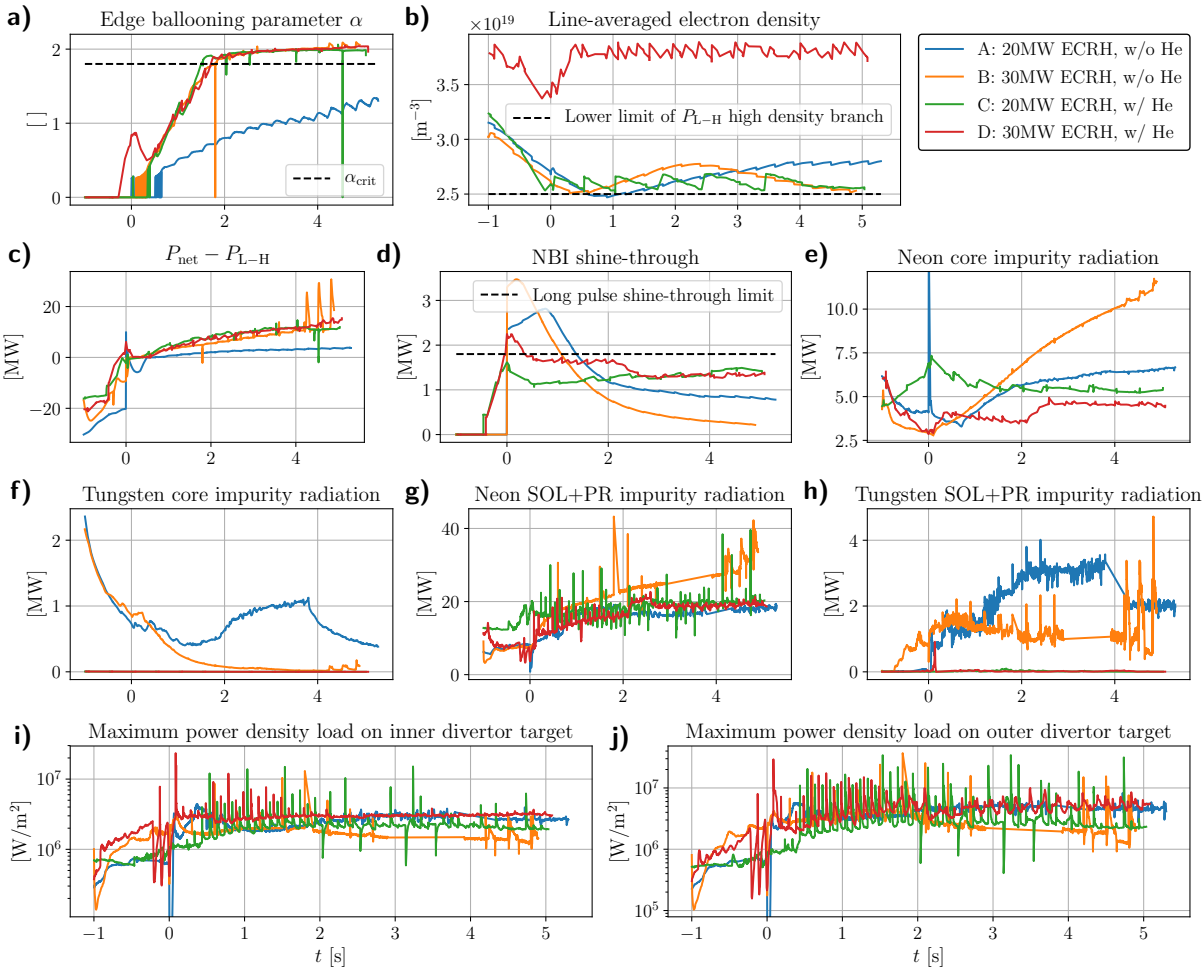

Figure 1: *Results of the hydrogen plasma simulations with JINTRAC. The horizontal axis in each of the plots is time [s], offset such that $t = 0$ is the start time of full auxiliary power injection. SOL+PR represents scrape-off layer plus private region. P_{net} in Fig. 1.c is defined as $P_{\mathrm{aux}} + P_{\mathrm{ohm}} - P_{\mathrm{rad}} - \mathrm{d}W_{\mathrm{p}}/\mathrm{d}t$.*

and a 15 % lowering of the $P_{\mathrm{L-H}}$ threshold due to the helium minority. In order to maintain the higher density regimes of case D, pellet fuelling was required, whereas the lower density cases were maintained by gas fuelling alone. Case C was assisted by pellet fuelling during the first few seconds of H-mode operation, but was maintained by gas puffing after $t \approx 3.5$ s.

Case B was excessively seeded with neon, with the shine-through power well below the long pulse shine-through limit (Fig. 1.d), and with neon core impurity radiation up to about 12 MW (and increasing) towards the end of the simulation (Fig. 1.e). The increasing radiation is due to continued neon seeding by gas puffing at a high rate. However, it has been demonstrated that case B can be safely transitioned to L-mode while ramping down in NBI power and plasma density, despite the large neon content. The details of this will be shown in a later publication.

Tungsten core and SOL radiation is small compared to neon in all four cases. Cases A and B have high tungsten core content during initial conditions compared to cases C and D, as

indicated by Fig. 1.f. The source of tungsten content and associated radiation in the scrape-off layer and private region in Fig. 1.h is supposedly a combination of sputtering from the divertor and diffusion of the initial condition core content for these cases. It should be noted that drifts in the SOL are disabled, only modelling particle transport by diffusion in this region, which affects impurity content predictions. Cases C and D show negligible tungsten radiation both in the core and in the SOL, indicating an insignificant source of tungsten from divertor sputtering.

Figures 1.i and 1.j show the maximum power density loads on the inner and outer divertor target plates, respectively. To ensure a sustained lifetime of the divertor, the maximum power load on the target plates should not stabilise above about 10 MW/m^2, preferably. The maximum power density is below this threshold in all four cases except for individual spikes that coincide with sawtooth crashes in the core.

Acknowledgements

JINTRAC was used under licence agreement between Euratom and CCFE, Ref. Ares(2014) 3576010-28/10/2014. This work was funded jointly by the RCUK Energy Programme [grant number EP/T012250/1] and by ITER Task Agreement C19TD53FE implemented by Fusion for Energy under Grant GRT-869 and Contract OPE-1057. The views and opinions expressed herein do not necessarily reflect those of the ITER Organization.

References

[1] "ITER Research Plan within the Staged Approach (Level III-Provisional version)", ITER Technical Report ITR-18-003 (2018). https://www.iter.org/technical-reports

[2] M. Schneider *et al.*, EPJ Web Conf. **157**, 03046 (2017)

[3] M. Romanelli *et al.*, Plasma Fusion Res. **9**, 3403023 (2014)

[4] Y.R. Martin *et al.*, J. Phys. Conf. Ser. **123**, 012033 (2008)

[5] E. Righi *et al.*, Nucl. Fusion **39**, 309 (1999)

[6] C.F. Maggi *et al.*, Nucl. Fusion **54**, 023007 (2014)

[7] E. Delabie *et al.*, 42nd EPS Conf. Plasma Phys. **39E**, O3.113 (2015)

[8] J. Hillesheim *et al.*, 26th IAEA Fusion Energy Conf., EX/5-2 (2016)

[9] E. Solano *et al.*, 47th EPS Conf. Plasma Phys, I1.104 (2021)

[10] M.J. Singh *et al.*, New J. Phys. **19**, 055004 (2017)

[11] D. Farina, Fusion Sci. Technol. **52**, 154 (2007)

[12] C.D. Challis *et al.*, Nucl. Fusion **29**, 563 (1989)

[13] L. Lauro-Taroni *et al.*, 21st EPS Conf. on Controlled Fusion Plasma Phys. **18B**, 102 (1994)

[14] G. Cenacchi and A. Taroni, 1988 JET-IR(88)03

[15] P.I. Strand *et al.*, 31st EPS Conf. Plasma Phys. **28G**, P-5.187 (2004)

[16] V. Parail *et al.*, Nucl. Fusion **49**, 075030 (2009)

[17] S. Wiesen, "EDGE2D/EIRENE code interface report", ITC project report 2005/6 (2006). http://www.eirene.de/e2deir_report_30jun06.pdf